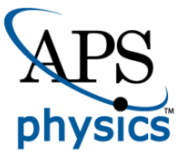

Is there evidence for sterile neutrinos in IceCube data?

V. Barger, Y. Gao, and D. Marfatia

Phys. Rev. D **85**, 011302 — Published 18 January 2012

DOI: 10.1103/PhysRevD.85.011302

Is there evidence for sterile neutrinos in IceCube data?

V. Barger[1], Y. Gao[2], D. Marfatia[3,1]

[1]*Department of Physics, University of Wisconsin, Madison, WI 53706, USA*
[2]*Department of Physics, University of Oregon, Eugene, OR 97403, USA*
[3]*Department of Physics and Astronomy, University of Kansas, Lawrence, KS 66045, USA*

Data from the LSND and MiniBooNE experiments, and revised expectations of the antineutrino flux from nuclear reactors suggest the existence of eV-mass sterile neutrinos. $3+2$ and $1+3+1$ scenarios accommodate all relevant short-baseline neutrino data except for the low-energy MiniBooNE anomaly. We analyze the angular distribution of upward going atmospheric neutrino events in the IceCube-40 dataset for evidence of sterile neutrinos within these scenarios. Depending on how systematic uncertainties are handled, we find strong evidence for, or weak evidence against sterile neutrinos. We show that future IceCube data will definitively settle the issue.

While oscillations of the three Standard Model neutrinos have been convincingly demonstrated, and the framework that explains the data of many disparate experiments is elegant in its simplicity, a nagging doubt persists. Are we seeing the effects of light sterile neutrinos in short-baseline neutrino (SBL) experiments? The question is raised by 3.3σ CL evidence from the Liquid Scintillator Neutrino Detector (LSND) [1] experiment for $\bar{\nu}_\mu \to \bar{\nu}_e$ oscillations with $L/E \sim 1$ m/MeV. This result is partially corroborated by the Mini-Booster Neutrino Experiment (MiniBooNE) [2]. The mass-squared difference $\delta m^2 \sim 1$ eV^2 indicated is very different from those that explain solar and atmospheric neutrino data. Since three neutrinos have only two independent mass-squared difference scales, a third δm^2 scale implies the existence of additional light neutrinos, which must be sterile because the invisible width of the Z boson requires that there be no more than three active neutrinos.

A new theoretical calculation of the $\bar{\nu}_e$ flux from nuclear reactors finds a value that is 3% higher than previous estimates [3]. If borne out, the incident flux at SBL reactor neutrino experiments may be interpreted as having a deficit due to oscillations into eV sterile neutrinos.

A recent analysis of SBL beam and reactor experiments, using the new reactor flux prediction, concludes that a $3+1$ scenario with a single additional eV sterile neutrino does not describe the data satisfactorily, while a $3+2$ scenario with two eV sterile neutrinos, and a $1+3+1$ scenario with one sterile neutrino lighter than the 3 active neutrinos and the other heavier, provide a good fit; see Table I for the best-fit parameters [4]. The phase $\delta \equiv arg(U_{\mu4}U^*_{e4}U^*_{\mu5}U_{e5})$, where U is the neutrino mixing matrix, leads to CP violation. Note that accommodating such eV sterile neutrinos in cosmology requires quite drastic modifications of ΛCDM [5].

The IceCube experiment (IC) [6] observes 10^5 atmospheric muon neutrino events per year thereby offering a unique probe of neutrino oscillations at energies above 100 GeV. For upward going neutrinos, any additional species that significantly mixes with ν_μ impacts the observed muon rate through ν_μ disappearance. In fact, for $\delta m^2 \sim 1$ eV^2, resonant oscillations are possible for TeV atmospheric neutrinos [7]. In its 40-string configuration, IC has observed 12877 atmospheric muon neutrino events in the energy range 332 GeV–84 TeV [8].

	δm^2_{41}	δm^2_{51}	$\lvert U_{e4}\rvert$	$\lvert U_{\mu4}\rvert$	$\lvert U_{e5}\rvert$	$\lvert U_{\mu5}\rvert$	δ/π
3+2	0.47	0.87	0.128	0.165	0.138	0.148	1.64
1+3+1(a)	-0.47	0.87	0.129	0.154	0.142	0.163	0.35
1+3+1(b)	0.47	-0.87	0.129	0.154	0.142	0.163	1.65

TABLE I. Global best-fit parameters to data from short-baseline experiments [4]. The two 1+3+1 cases correspond to either m_4 or m_5 being the lightest state. The active neutrinos have a normal hierarchy, and $\theta_{13} = 0$.

In this Letter, we analyze the zenith-angle distribution of the IC data to see if it provides supporting evidence for sterile neutrino explanations of the SBL data and the reactor antineutrino anomaly as encapsulated by the scenarios of Table I, and assess the future sensitivity of the IC detector. The energy window of the IC dataset is optimal as can be seen from Fig. 1. We expect IC data to not be very sensitive to the $3+2$ case since the resonance occurs in the $\bar{\nu}_\mu$ channel which is subdominant in the atmospheric flux. In the $1+3+1$ cases, the dominant ν_μ flux is also suppressed so that these cases can be discriminated more readily from the 3ν case.

The muon events at IC can be classified as (i) 'contained' events, namely events with muon tracks that start within the instrumented volume, and (ii) 'up-going' events in which the muon is produced outside the detector. See Eqs. 8 and 10 of Ref. [10] for details and note that the incident ν_μ flux includes a contribution from $\nu_e \to \nu_\mu$ oscillations.

For the points in Table I, the muon neutrino flux is suppressed by $\sim 10\%$ above 100 GeV, with a corresponding reduction in the muon event rate. Thus, the 25% uncertainty in the atmospheric neutrino flux [11] is a serious impediment to a rate analysis. Instead, a distortion in the zenith-angle distribution of the detected muons would provide the strongest evidence for sterile neutrinos. As most sub-TeV neutrinos do not distort the angular distribution, useful information may be extracted from high-energy events. It so happens that the cut at 332 GeV

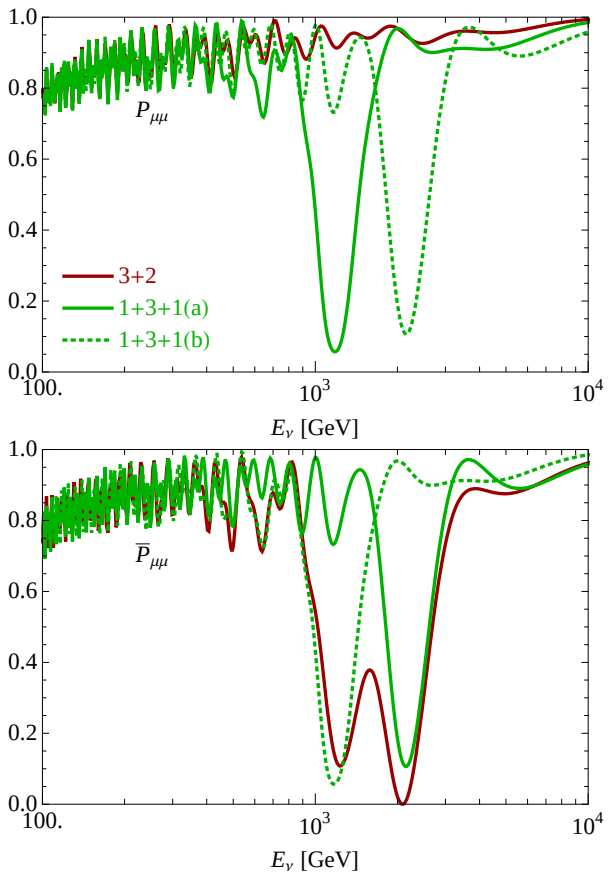

FIG. 1. The survival probability for ν_μ (upper panel) and $\bar{\nu}_\mu$ (lower panel) for vertically going upward neutrinos ($\cos\theta_z = -1$) in the 3 scenarios of Table I. We use the density profile of the Preliminary Reference Earth Model [9].

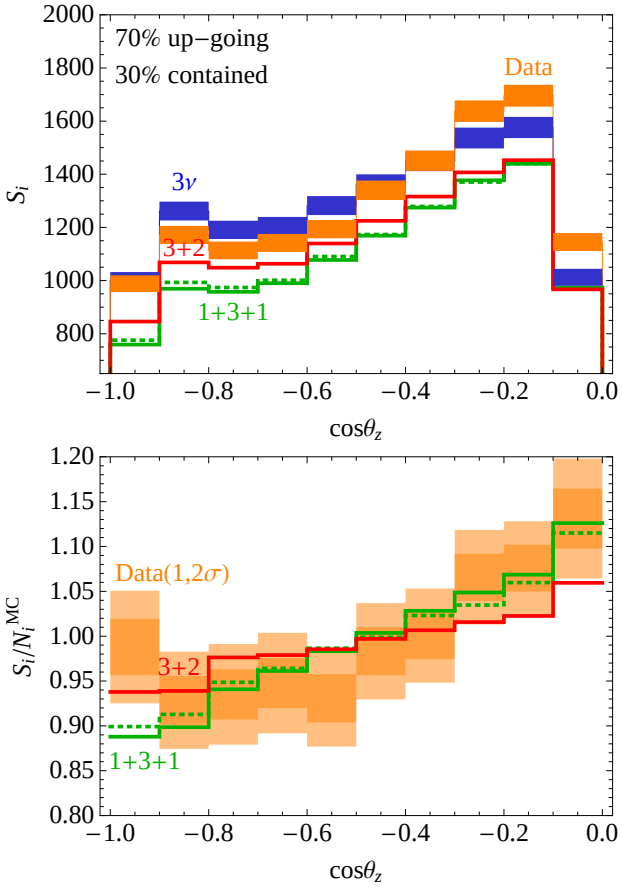

FIG. 2. Upper panel: Zenith-angle distributions for muon events at IC. The IC data (light, orange) and the expectation for 3ν oscillations (dark, blue) are shown with 2σ statistical uncertainty bands. The expectations for the $3+2$ (dark, red), $1+3+1$(a) (light, green solid), and $1+3+1$(b) (light, green dotted) scenarios are shown. We set $a = 1\,, b = 0$ to display the rate suppression and the spectral shape in each case. Lower panel: Relative distortion of the zenith-angle spectra in comparison to the expectation for 3ν oscillations. Here, the best-fit value of a is used in each case, but $b = 0$. The data reveal an obvious distortion with respect to the 3ν expectation.

suppresses 90% of sub-TeV muon events while leaving a large sample of 10^4 events.

To make it to the detector, up-going muons can travel at most the stopping distance which increases with energy. As a result, the effective volume for neutrinos is larger for high energy neutrinos that more readily produce energetic muons. In turn, the up-going sample has a larger fraction of high-energy events than the contained sample, making it particularly valuable in an analysis of the zenith-angle distribution. The 40-string IC data consist of 70% up-going and 30% contained events [12].

To account for experimental efficiencies, we determine the theoretical zenith-angle spectrum as in Ref. [13]:

$$S_i^{th} = a[1 + b((\cos\theta_z)_i + 0.5)]\frac{N_i^{MC}}{N_i^{3\nu}}N_i^{th}\,, \qquad (1)$$

where N_i^{th} is the number of muon events in angular bin i, and $N_i^{MC}/N_i^{3\nu}$ is a bin-wise factor that scales our theoretical 3ν prediction to IceCube's Monte Carlo [8]. a is an overall normalization and b allows a systematic tilt of the spectrum. Both parameters are allowed to float in a χ^2 analysis. Note that $S_i^{th} = N_i^{MC}$ in the 3ν case with $a = 1\,, b = 0$.

The upper panel of Fig. 2 illustrates the event rate suppression and zenith-angle distributions in the scenarios under consideration. The large difference of the sterile neutrino scenarios from the IC data and from the 3ν expectation in the near-vertical ($-1.0 \le \cos\theta_z \le -0.9$) bin promises much discriminating power. The near-horizon ($-0.1 \le \cos\theta_z \le 0$) bin has potentially large systematic errors from the misidentification of coincident downward events as horizontal events, and we do not include it in our χ^2 analysis. For our analyses we define

$$\chi^2 = \frac{(1-a)^2}{\sigma_a^2} + \sum_i \frac{(S_i^{th} - S_i^{exp})^2}{S_i^{exp}}\,, \qquad (2)$$

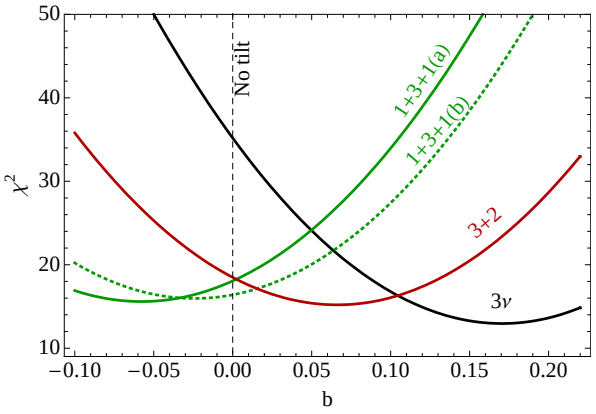

FIG. 3. χ^2 as a function of the tilt parameter b from a fit to the 9 zenith-angle bins of Fig. 2 with $\cos\theta_z < -0.1$.

	no tilt ($b = 0$)	tilted	
	χ^2	χ^2	b
3ν	35.2	13.0	0.17
$3+2$	18.5	15.2	0.066
$1+3+1$(a)	18.1	15.6	-0.058
$1+3+1$(b)	16.4	16.0	-0.024

TABLE II. Best-fit χ^2 and b from the curves in Fig. 3. Without a systematic tilt in the angular distribution, sterile neutrino scenarios are clearly favored over the 3ν case. If a large systematic tilt is permissible, the sterile cases are mildly disfavored. For $|b| < 0.11$, all scenarios give a comparable fit.

where $\sigma_a = 0.25$ is the percent uncertainty in the atmospheric flux normalization [11] and S^{exp} denotes either real or simulated data. In what follows, we always fit a, and either set $b = 0$ or marginalize over b without penalty. The lower panel of Fig. 2 shows the spectral distortion of the IC data and the sterile neutrino scenarios relative to 3ν oscillations. In the latter case, $a = 1\,, b = 0$, while the best-fit value of a is used for the sterile cases with $b = 0$.

The results of fitting the 9 non-horizontal ($\cos\theta_z < -0.1$) bins are shown in Fig. 3 and Table II. The 3ν scenario gives a better fit provided the data are plagued by a large systematic tilt. If $|b|$ is restricted to be smaller than 0.11, the 3ν fit yields a χ^2 of 15.8, which is comparable to the values ($\sim$ 15–16) of the sterile neutrino cases.

A natural question is if there are correlated signals in cascade events at IC. Interestingly, above 332 GeV, we find a comparable total number of ν_e plus ν_τ events/km^3/year in the 3ν ($\sim$ 890) and sterile neutrino ($\sim$ 850) cases. The corresponding number of induced cascade events can be obtained by folding with the IC efficiency which is not available to us.

That future IC data with systematics under control have the ability to reveal a deviation due to sterile neutrinos is evident from Fig. 4. The monotonically rising event ratio as a function of $\cos\theta_z$ in the up-going event sample is a striking signature of sterile neutrino oscil-

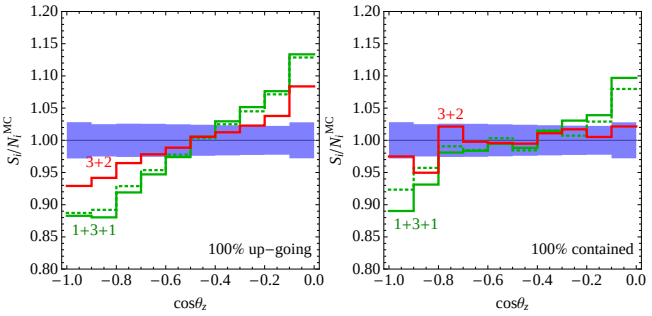

FIG. 4. Similar to the lower panel of Fig. 2, but with 1.3×10^5 events above 332 GeV equipartitioned into purely up-going events (left panel) and purely contained events (right panel). The shaded band represents the 2σ statistical uncertainty on the 3ν expectation. Sterile neutrino scenarios will be easily distinguishable from 3ν oscillations from the up-going event sample.

lations. On the other hand, strong exclusions can also be obtained. Assuming a sample of 6.5×10^4 up-going events with no deviation from the 3ν result, and fitting to all 10 angular bins with only a varied yields $\chi^2 = 111$, 386 and 331 for the $3+2$, $1+3+1$(a) and (b) cases, respectively, compared to a $\chi^2 \sim 10$ for 3ν oscillations. An interesting aspect of the contained event sample is that in all cases the zenith-angle distribution is almost flat for $-0.8 < \cos\theta_z < -0.2$ so that the features in the near-vertical and near-horizon bins are insensitive to a systematic tilt. With 6.5×10^4 contained events, we find $\chi^2 = 28$, 165 and 87 for the $3+2$ and $1+3+1$(a) and (b) cases, respectively. With such sensitivity IC will easily confirm or exclude sterile neutrino scenarios.

Acknowledgments. We thank S. Grullon, F. Halzen, W. Huelsnitz, J. Koskinen, B. Louis, S. Pakvasa and T. Schwetz for useful discussions and correspondence. VB thanks the KITP, UCSB for its hospitality. DM thanks the University of Hawaii for its hospitality during the completion of this work. This research was supported by DOE grants DE-FG02-96ER40969, DE-FG02-95ER40896 and DE-FG02-04ER41308, and NSF grants PHY-0544278 and PHY05-51164.

[1] A. Aguilar *et al.* [LSND Collaboration], Phys. Rev. D **64**, 112007 (2001) [arXiv:hep-ex/0104049].
[2] A. A. Aguilar-Arevalo *et al.* [MiniBooNE Collaboration], Phys. Rev. Lett. **105**, 181801 (2010) [arXiv:1007.1150 [hep-ex]].
[3] T. A. Mueller *et al.*, Phys. Rev. C **83**, 054615 (2011)

[arXiv:1101.2663 [hep-ex]].
[4] J. Kopp, M. Maltoni, T. Schwetz, arXiv:1103.4570 [hep-ph].
[5] J. Hamann, S. Hannestad, G. G. Raffelt, Y. Y. Y. Wong, [arXiv:1108.4136 [astro-ph.CO]].
[6] T. K. Gaisser [for the IceCube Collaboration], arXiv:1108.1838 [astro-ph.HE].
[7] M. V. Chizhov, S. T. Petcov, Phys. Rev. **D63**, 073003 (2001) [hep-ph/9903424]; H. Nunokawa, O. L. G. Peres, R. Zukanovich Funchal, Phys. Lett. **B562**, 279-290 (2003) [arXiv:hep-ph/0302039]; S. Choubey, JHEP **0712**, 014 (2007) [arXiv:0709.1937 [hep-ph]].
[8] R. Abbasi *et al.* [IceCube Collaboration], arXiv:1104.5187 [astro-ph.HE].
[9] A. M. Dziewonski, D. L. Anderson, Phys. Earth Planet. Interiors **25**, 297-356 (1981).
[10] V. Barger, Y. Gao, D. Marfatia, Phys. Rev. **D83**, 055012 (2011) [arXiv:1101.4410 [hep-ph]].
[11] M. Honda, T. Kajita, K. Kasahara, S. Midorikawa, T. Sanuki, Phys. Rev. D **75**, 043006 (2007) [arXiv:astro-ph/0611418].
[12] S. Grullon, private communication.
[13] S. Razzaque, A. Y. Smirnov, JHEP **1107**, 084 (2011) [arXiv:1104.1390 [hep-ph]].